

# Stagnation Point Flow Over a Stretching or Shrinking Cylinder in a Copper-Water Nanofluid

Noor Syamimi Omar, Norfifah Bachok and Norihan Md. Arifin

Department of Mathematics and Institute for Mathematical Research, University Putra Malaysia, 43400 UPM Serdang, Selangor-43400, Malaysia

## Abstract

The problem of steady stagnation-point flow over a stretching or shrinking cylinder in a water-based Copper (Cu) nanofluid is considered in this study. The governing partial differential equations in cylindrical form are reduced to ordinary differential equations using a similarity transformation. The resulting system is solved numerically by using shooting method with Prandtl number  $Pr = 6.2$ . The skin friction coefficient, Nusselt number, and the velocity and temperature profiles are presented graphically and discussed. The governing equation of the problem shows that the flow and heat transfer characteristics depend on the effects of the curvature parameter, stretching or shrinking parameter and nanoparticle volume fraction parameter. It is found that the solutions for a shrinking cylinder are non-unique which differ from a stretching cylinder. It is observed that the surface shear stress and the heat transfer rate at the surface increase as the curvature parameter increases.

**Keywords:** Boundary Layer, Dual Solutions, Nanofluid, Stagnation Point, Stretching or Shrinking Cylinder

## 1. Introduction

The study on stagnation point flow and heat transfer over a stretching or shrinking sheet has gained considerable attention due to its applications in industries and important bearings on several technologies processes, for examples in the extrusion of plastic sheets, paper production, glass blowing, metal spinning, drawing plastic films (Locket al.<sup>1</sup>). The stagnation region encounters the highest pressure, highest heat transfer and highest rate of mass deposition. Thus, the most desired characteristics are depends on the rate of cooling in the process and the process of stretching/shrinking. The problem of two-dimension stagnation flow towards a stationary semi-infinite wall was first studied by Hiemenz<sup>2</sup>, using similarity transformation, to reduce the Navier-Stoke equations to nonlinear ordinary differential equations. Then, the problem was extended

by Homann<sup>3</sup> to the case of axisymmetric stagnation-point flow. Mahapatra & Gupta<sup>4</sup> studied the combination of both stagnation-point flows past a stretching surface. Wang<sup>5</sup> studied the stagnation flow towards a shrinking sheet which considered both two-dimensional and axisymmetric stagnation flows. Then, he studied the natural convection on a vertically radially stretching sheet (Wang<sup>6</sup>). After this pioneering work, the flow field over a stagnation point towards a stretching/shrinking sheet has drawn many interests to the researchers such as Bachok et al.<sup>7</sup>, Bhattacharyya<sup>8</sup> and Locket al.<sup>9</sup>.

All studies mentioned above refer to the stagnation point flow towards a stretching/shrinking sheet in a viscous and Newtonian-fluid. This paper consider the problem of steady boundary layer flow, heat transfer, and nanoparticle fraction over a stagnation point flow towards a stretching or shrinking cylinder in a nanofluid, with

\* Author for correspondence

water as the based fluid. Flow over cylinders is considered to be two-dimensional if the body-radius is large compared to the boundary layer thickness. Meanwhile, for a thin or slender cylinder, the radius of the cylinder may be of the same order as that of the boundary layer thickness. Thus, the flow may be considered as axi-symmetric instead of two-dimensional (Ishaket al.<sup>10</sup>, Mukhopadhyay<sup>11</sup>, Poply<sup>12</sup>, Vajraveluet al.<sup>13</sup> and Najibet al.<sup>14</sup>). Nanofluids are highly potential fluid in heat transfer enhancement and have wide applications in industrial application such as electronics, nuclear reactor, drying processes, heat exchanger, geothermal, oil recovery and many more as stated by Ahmad & Pop<sup>15</sup>. The comprehensive references on nanofluids can be found in review papers by Rohnket al.<sup>16</sup>, Bachoket al.<sup>17</sup> and Popaet al.<sup>18</sup>. In advance, this study may be regarded as the extension of the papers by Hiemenz<sup>2</sup>, Wang<sup>5</sup> and Bachoket al.<sup>19</sup> from a flat plate to a cylinder surface. Thus, the results obtained can be compared, if the curvature parameter is neglected.

## 2. Basic Equations

Consider a steady stagnation-point flow towards a horizontal linearly stretching or shrinking cylinder with radius  $R$  placed in a Cu-water fluid of constant temperature  $T_w$ . It is assumed that the free stream and the stretching/shrinking velocities are  $u_\infty(x) = U_\infty x/L$  and  $u_w(x) = U_w x/L$  respectively. The boundary layer equations are,

$$\frac{\partial}{\partial x}(ru) + \frac{\partial}{\partial r}(rv) = 0 \tag{1}$$

$$u \frac{\partial u}{\partial x} + v \frac{\partial u}{\partial r} = u_\infty \frac{du_\infty}{dx} + \frac{\mu_{nf}}{\rho_{nf}} \left( \frac{\partial^2 u}{\partial r^2} + \frac{1}{r} \frac{\partial u}{\partial r} \right) \tag{2}$$

$$u \frac{\partial T}{\partial x} + v \frac{\partial T}{\partial r} = \alpha_{nf} \left( \frac{\partial^2 T}{\partial r^2} + \frac{1}{r} \frac{\partial T}{\partial r} \right) \tag{3}$$

subject to boundary equations,

$$\begin{aligned} u &= u_w(x), \quad v = 0, \quad T = T_w \quad \text{at } r = R, \\ u &\rightarrow u_\infty(x), \quad T \rightarrow T_\infty \quad \text{as } r \rightarrow \infty \end{aligned} \tag{4}$$

Where  $x$  and  $r$  are coordinates measured along the surface of the cylinder and in the radial direction, respectively, with  $u$  and  $v$  being the corresponding velocity components. Further,  $T$  is the temperature of the nanofluid,  $\mu_{nf}$  is the viscosity of the nanofluid,  $\alpha_{nf}$  is the thermal diffusivity of the nanofluid, which are given by Oztop & Abu-Nada<sup>20</sup>

$$\begin{aligned} \alpha_{nf} &= \frac{k_{nf}}{(\rho C_p)_{nf}}, \quad \rho_{nf} = (1-\varphi)\rho_f + \varphi\rho_s, \quad \mu_{nf} = \frac{\mu_f}{(1-\varphi)^{2.5}} \\ (\rho C_p)_{nf} &= (1-\varphi)(\rho C_p)_f + \varphi(\rho C_p)_s, \quad \frac{k_{nf}}{k_f} = \frac{(k_s + 2k_f) - 2\varphi(k_f - k_s)}{(k_s + 2k_f) + \varphi(k_f - k_s)} \end{aligned} \tag{5}$$

Here,  $\varphi$  is the nanoparticle volume fraction,  $(\rho C_p)_{nf}$  is the heat capacity of the nanofluid,  $k_{nf}$  is the thermal conductivity of the nanofluid,  $k_f$  and  $k_s$  are the thermal conductivities of the fluid and the solid fractions, respectively.  $\rho_f$  and  $\rho_s$  are the densities of the fluid and densities of the solid fractions, respectively. It should be mention that the use of  $k_{nf}/k_f$  expression is restricted only for spherical nanoparticles which other shapes of nanoparticles are not valid.

We look for similarity solutions of equations (1)-(3), subject to the boundary conditions (4), by introducing the following transformation,

$$\eta = \frac{r^2 - R^2}{2R} \left( \frac{u_\infty}{\nu x} \right)^{1/2}, \quad \psi = (\nu x u_\infty)^{1/2} R f(\eta), \quad \theta(\eta) = \frac{T - T_\infty}{T_w - T_\infty} \tag{6}$$

Where  $\eta$  is the similarity variable and  $\Psi$  is the stream function defined as  $u = r^{-1} \partial \Psi / \partial r$  and  $v = -r^{-1} \partial \Psi / \partial x$ , which identically satisfies equation (1). By employing the similarity variables (6), equations (2) and (3) are reduced to the following ordinary differential equations,

$$\frac{1}{(1-\varphi)^{2.5} (1-\varphi + \varphi\rho_s/\rho_f)} [(1+2\gamma\eta) f''' + 2\gamma f' f''] + f f'' - f'^2 + 1 = 0 \tag{7}$$

$$\frac{1}{Pr} \left[ \frac{k_{nf}/k_f}{1-\varphi + \varphi(\rho C_p)_s/(\rho C_p)_f} \right] [(1+2\gamma\eta) \theta'' + 2\gamma\theta'] + f\theta' = 0 \tag{8}$$

subject to the boundary conditions (4) which become,

$$\begin{aligned} f(0) &= 0, \quad f'(0) = \varepsilon, \quad \theta(0) = 1, \\ f'(\infty) &\rightarrow 1, \quad \theta(\infty) \rightarrow 0 \end{aligned} \tag{9}$$

where  $\gamma$  is the curvature parameter and Pr is the Prandtl number defined respectively as,

$$\gamma = \left( \frac{\nu_f L}{U_\infty R^2} \right)^{1/2}, \quad Pr = \frac{\nu}{\alpha} \tag{10}$$

and  $\varepsilon = U_w/U_\infty$  is stretching or shrinking parameter,  $\varepsilon > 0$  is for stretching and  $\varepsilon < 0$  is for shrinking.

The physical quantities of interest are the skin friction coefficient  $C_f$  and the local Nusselt number  $Nu_x$ , which are defined as,

$$C_f = \frac{\tau_w}{\rho_f u_\infty}, \quad Nu_x = \frac{x q_w}{k_f (T_w - T_\infty)} \tag{11}$$

where the surface shear stress  $\tau_w$  and the surface heat transfer flux  $q_w$  are given by,

$$\tau_w = \mu_{nf} \left( \frac{\partial u}{\partial r} \right)_{r=R}, \quad q_w = -k_{nf} \left( \frac{\partial T}{\partial r} \right)_{r=R}, \quad (12)$$

using the similarity variables (6), we obtain,

$$C_f \text{Re}_x^{1/2} = \frac{1}{(1-\varphi)^{2.5}} f''(0), \quad (13)$$

$$\text{Nu}_x \text{Re}_x^{-1/2} = -\frac{k_{nf}}{k_f} \theta'(0), \quad (14)$$

Where,  $\text{Re}_x = u_\infty x / V_f$  is the local Reynolds number.

### 3. Results and Discussion

Numerical solutions to the ordinary differential equations (7) and (8) with the boundary conditions (9) were obtained using shooting method. The dual solutions were obtained by setting different initial guesses for the missing values of  $f''(0)$  and  $-\theta'(0)$ , where all profiles satisfy the boundary condition (9) asymptotically but with different shapes. The effect of the solid volume fraction  $\varphi$  and curvature parameter  $\gamma$  are analyzed for (Cu)-water nanofluid. Following Oztop & Abu-Nada<sup>20</sup> the value of the Prandtl number Pr is taken as 6.2 (water) and the volume fraction ( $0 \leq \varphi \leq 0.2$ ) in which  $\varphi=0$  corresponds to the regular fluid. The thermophysical properties of the fluid and the nanoparticle, copper, are listed in Table 1. Comparisons with previously reported data by Bachok et al.<sup>19</sup> are made for several values of  $\varepsilon$  and  $\gamma$  as presented in Table 2, and thus give confidence that the numerical results obtained are accurate. In addition, the values of  $f''(0)$  for  $\gamma=0.2$  and  $0.4$  are also listed in Table 2 for future references.

**Table 1.** Thermo physical properties of fluid and nanoparticles (Oztop& Abu-Nada20)

Physical properties	Fluid phase (water)	Cu
$C_p$ (J/kg K)	4179	385
$\rho$ (kg/m <sup>3</sup> )	997.1	8933
$k$ (W/mK)	0.613	400

The variations of  $f''(0)$  and  $-\theta'(0)$  with  $\varepsilon$  are shown in Figures 1 and 2 for some values of the curvature parameter  $\gamma$ . These figures show that there are regions of

unique solutions for  $\varepsilon \geq -1$ , dual solutions for  $\varepsilon_c < \varepsilon < -1$  and no solutions for  $\varepsilon < \varepsilon_c < -1$ . Based on our computation, the critical value of  $\varepsilon$  (say  $\varepsilon_c$ ), which show a favorable agreement with the previous investigations for the case  $\gamma = 0$  (flat plate) in Bachok et al.<sup>19</sup> is shown in Table 3. Furthermore, the result in Figure 1 also indicates that as the curvature parameter  $\gamma$  increases, the skin friction coefficient  $f''(0)$  is increases too. The range of  $\varepsilon$  for which the solution exists is larger for  $\gamma > 0$  (cylinder) compared to  $\gamma = 0$ . Thus, this demonstrates that a cylinder increases the range of existence of the similarity solution to the equations 7-9 compared to the flat plate. In addition, the boundary layer separation is delayed for a cylinder<sup>18</sup>. Figure 2 illustrate the initial value- $\theta'(0)$  which proportional to the heat loss from the surface, increases with an increase of  $\gamma$ . Since the boundary layer become becomes thicker as shrinking is increased, the heat transfer rate at the surface decreases accordingly.

**Table 2.** Values of  $f''(0)$  for some values of  $\varepsilon$  and  $\gamma$

$\varepsilon$	Bachok et al <sup>19</sup>		Present results	
	$\varphi=0.1$		$\varphi=0.1$	
	$\gamma=0$	$\gamma=0$	$\gamma=0.2$	$\gamma=0.4$
2	-2.217106	-2.217106	-2.307873	-2.396084
1	0	0	0	0
0.5	0.837940	0.837940	0.887754	0.935394
0	1.447977	1.447977	1.553805	1.653867
-0.5	1.757032	1.757022	1.933203	2.096118
-1	1.561022	1.561022	1.866443	2.127965
	[0]	[0]	[0]	[0]
-1.15	1.271347	1.271347	1.684248	2.003737
	[0.137095]	[0.137095]	[-0.026540]	[-0.131198]
-1.2	1.095419	1.095419	1.590181	1.939265
	[0.274479]	[0.274479]	[0.028451]	[-0.101872]
-1.2465	0.686379	0.686380	1.478323	1.865189
	[0.651161]	[0.651160]	[0.109422]	[-0.052290]

“[ ]” second solution

Figure 3 and 4 illustrate the variations of the skin friction coefficient and the local Nusselt number, given by equations (13) and (14) with the curvature parameter  $\gamma$  and the nanoparticle volume fraction parameter  $\varphi$ . These figures show that these quantities are increase almost linearly with  $\varphi$  and  $\gamma$ . These figures also indicate that as the curvature parameter  $\gamma$  increases, the skin friction coefficient and the local Nusselt number also increases. It

shows that presence of the nanoparticle, copper, in the fluid increases appreciably the effective thermal conductivity of the fluid and consequently enhances the heat transfer characteristics. The numerical values of  $C_f Re_x^{1/2}$  and  $Nu_x Re_x^{1/2}$  for some value of  $\gamma$  and  $\varphi$  are presented in Table 4 and 5, which show favorable agreement with previous study for the case  $\varepsilon=0.5$  for Cu-water in Bachoket al.<sup>19</sup>.

**Table 3.** Variation of  $\varepsilon_c$  with curvature parameter  $\gamma$

$\gamma$	Bachok et al <sup>19</sup>	Present results
0	-1.2465	-1.24657
0.2		-1.36252
0.4		-1.46180

**Table 4.** Values of  $C_f Re_x^{1/2}$  for some values of  $\gamma$  and  $\varphi$  with  $\varepsilon = 0.5$

$\gamma$	$\varphi$	Bachok et al <sup>19</sup>	Present results
0	0		0.7133
	0.05		0.8992
	0.1	1.0904	1.0904
	0.15		1.2945
	0.2	1.5177	1.5177
0.2	0		0.7629
	0.05		0.9557
	0.1		1.1553
	0.15		1.3693
	0.2		1.6049
0.4	0		0.8101
	0.05		1.0097
	0.1		1.2173
	0.15		1.4409
	0.2		1.6882

Figures 5 and 6 illustrate the velocity and temperature profiles for some value of  $\gamma$ . These Figures show that the boundary layer thickness for the upper branch solutions is smaller than the lower branch solutions. Figure 7-10 show the variations of the velocity and temperature profiles for different values of  $\varphi$  and  $\varepsilon$ . These Figures show that the far-field boundary condition (9) are satisfied, and thus support the validity of the numerical results obtained. It should be mentioned that the first solutions are stable, while the second solutions are not.

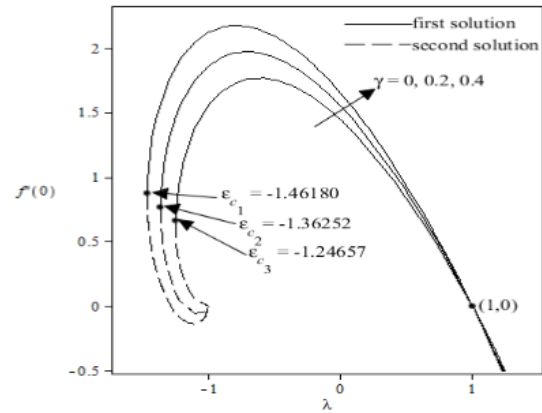


**Figure 1.** Variation of  $f''(0)$  with  $\varepsilon$  for some values of  $\gamma$  with  $\varphi = 0.1$ .

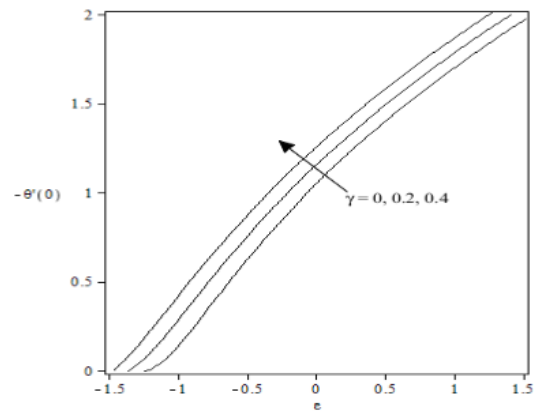


**Figure 2.** Variation of  $-\theta'(0)$  with  $\varepsilon$  for some values of  $\gamma$  with  $\varphi = 0.1$ .

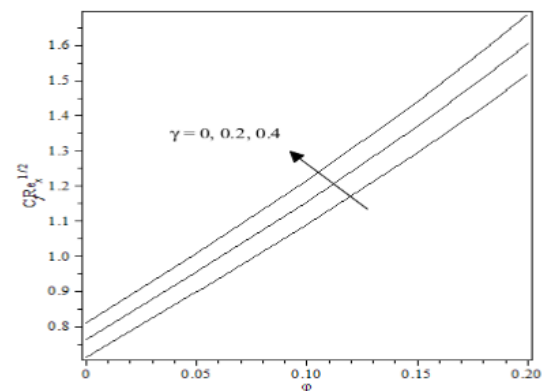


**Figure 3.** Variation of the skin friction coefficient for different value of  $\gamma$  with  $\varepsilon = 0.5$ .

**Table 5.** Values of  $Nu_x Re_x^{1/2}$  for some values of  $\gamma$  and  $\varphi$  with  $\varepsilon = 0.5$

$\gamma$	$\varphi$	Bachok et al <sup>19</sup>	Present results
0	0		1.5954
	0.05		1.7338
	0.1	1.8724	1.8724
	0.15		2.0131
0.2	0.2	2.1577	2.1577
	0		1.6895
	0.05		1.8415
	0.1		1.9953
0.4	0.15		2.1533
	0.2		2.3171
	0		1.7806
	0.05		1.9458
0.1	0.1		2.1143
	0.15		2.2887
	0.2		2.4709
	0.2		2.4709

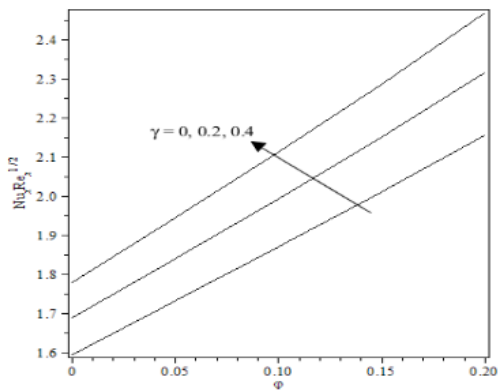


**Figure 4.** Variation of the local Nusselt number  $Nu_x Re_x^{1/2}$  for different value of  $\gamma$  with  $\varepsilon = 0.5$ .

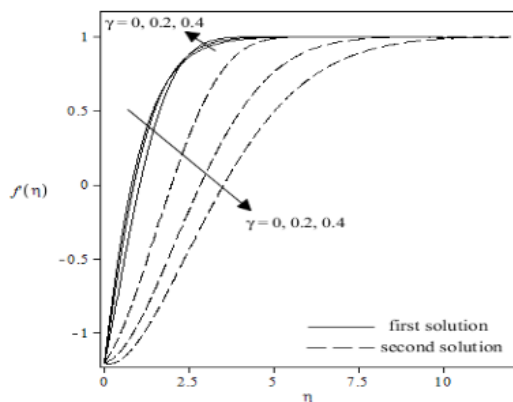


**Figure 5.** Velocity profiles for some values of  $\gamma$  with  $\varphi = 0.1, \varepsilon = -1.2$ .

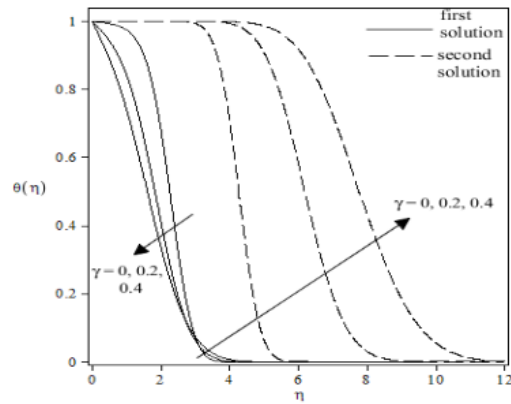


**Figure 6.** Temperature profiles for some values of  $\gamma$  with  $\varphi = 0.1, \varepsilon = -1.2$ .

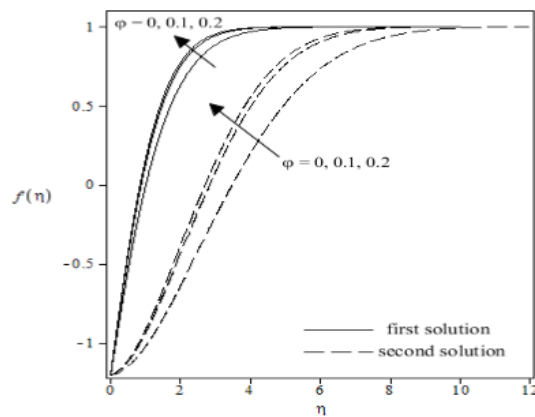


**Figure 7.** Velocity profiles for some values of  $\varphi(0 \leq \varphi \leq 0.2)$  with  $\gamma = 0.2, \varepsilon = -1.2$ .

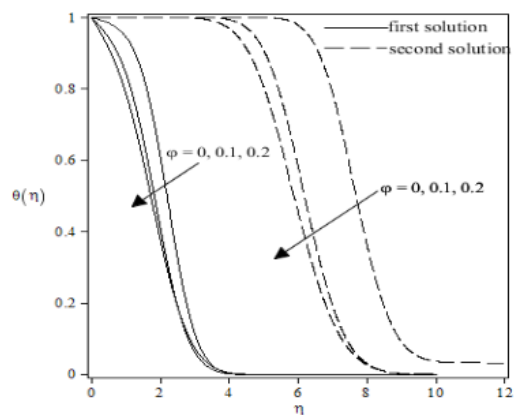


**Figure 8.** Temperature profiles for some values of  $\varphi(0 \leq \varphi \leq 0.2)$  with  $\gamma = 0.2, \varepsilon = -1.2$ .

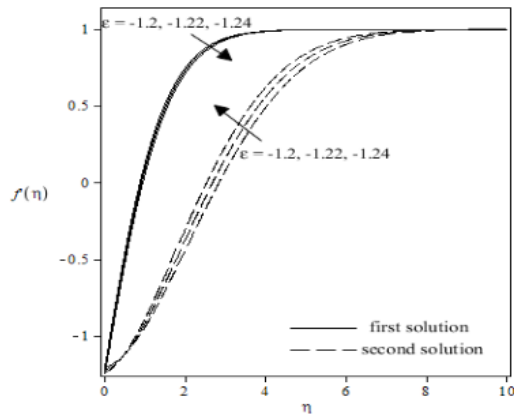


**Figure 9.** Velocity profiles for some values of  $\epsilon$  with  $\gamma = 0.2$  and  $\phi = 0.1$ .

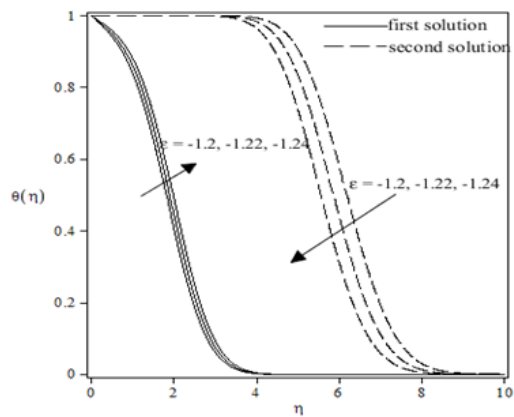


**Figure 10.** Temperature profiles for some values of  $\epsilon$  with  $\gamma = 0.2$  and  $\phi = 0.1$ .

## 4. Conclusion

We have theoretically studied how the governing parameters, namely curvature parameter  $\gamma$ , stretching/shrinking parameter  $\epsilon$  and the solid volume fraction  $\phi$  influence the boundary layer flow and the heat transfer characteristic on the surface of a horizontal cylinder. When  $\gamma = 0$ , the problem under consideration reduces to the flat plate case considered by the previous studies. Different from a stretching cylinder, it is found that the solutions for a shrinking cylinder are non-unique. The inclusion of nanoparticle, copper, into the base water fluid has increases the skin friction and heat transfer coefficients. The heat transfer rate increases as the solid volume fraction  $\phi$  increases. Further, it was found that increasing the curvature parameter  $\gamma$  is to increase the surface shear stress and the heat transfer rate at the surface.

## 5. Acknowledgement

The financial supports received from the Ministry of Higher Education, Malaysia (Project code: FRGS/1/2012/SG04/UPM/03/1) and the Research University Grant (RUGS) from the Universiti Putra Malaysia are gratefully acknowledgement.

## 6. References

1. Lok YY, Merkin JH, Pop I. Mixed convection flow near the axisymmetric stagnation point on a stretching or shrinking sheet. *Int J Therm Sci.* 2012; 59:186–94.
2. Heimenz K. Die Grenzschicht an einem in den gleichformig keitsstromeingetauchtengeradenkreiszyliner. *Dingler's Polytech J.* 1911; 326:321–4.
3. Homann F. Der einfluss grosser zahigkeitbei der strömung um den zylinder und um die kugel. *Zeitschrift Angewandte Math Mech.* 1936; 13:153–64.
4. Mahapatra TR, Gupta AS. Stagnation-point flow towards a stretching surface. *The Can J Chem Engng.* 2003; 81:258–63.
5. Wang CY. Stagnation flow towards a shrinking sheet. *Int J Non-linear Mech.* 2008; 43:377–82.
6. Wang CY. Natural convection on a vertical radially stretching sheet. *J Math Analysis Appl.* 2007; 332:877–83.
7. Bachok N, Ishak A, Pop I. Melting heat transfer in boundary layer stagnation–point flow towards a stretching/shrinking sheet. *Phy Letter A.* 2010; 374:4075–9.
8. Bhattacharyya K. Dual solutions in unsteady stagnation–point flow over a shrinking sheet. *Chi Phys Soc.* 2011; 28(8):1–4.
9. Lok YY, Ishak A, Pop I. MHD stagnation point flow with suction towards a shrinking sheet, *Sains Malaysiana.* 2011; 40(10):1179–86.
10. Ishak A, Nazar R, Pop I. Uniform suction/blowing effect on flow and heat transfer due to a stretching cylinder. *Appl Math Model. Model.* 2008; 32:2059–66.
11. Mukhopadhyay S. MHD boundary layer slip flow along a stretching cylinder. *Ain Shams Eng J.* 2013; 4:317–24.
12. Poply V, Singh P, Chaudhary KK. Analysis of laminar boundary layer flow along a stretching cylinder in the presence of thermal radiation. *WSEAS Trans Fluid Mech.* 2013;4:159–64.
13. Vajravelu K, Prasad KV, Santhi SR, Umesh V. Fluid flow and heat transfer over a permeable stretching cylinder. *J Appl Fluid Mech.* 2014; 7:111–20.
14. Najib N, Bachok N, Arifin NM, Ishak A. Stagnation point flow and mass transfer with chemical reaction past a stretching/shrinking cylinder. *Appl Math Chem Eng.* 2014;4:1–7.
15. Ahmad S, Pop I. Mixed convection boundary layer flow from a vertical flat plate embedded in a porous medium filled with nanofluid. *Int Comm Heat Mass Transf.* 2010; 37:987–91.
16. Rohni AM, Ahmad S, Pop I. Boundary layer flow over a moving surface in za nanofluid beneath a uniform free

- stream. *Int J Num Meth Heat Fluid Flow*. 2011; 21(7): 828–46.
17. Bachok N, Ishak A, Pop I. Boundary layer stagnation–point flow and heat transfer over an exponentially stretching/shrinking sheet in a nanofluid. *Int J Heat Mass Transf*. 2012; 55:8122–8.
  18. Popa CV, Kasaean AB, Nasiri S, Korichi A, Polidori G. Natural convection heat and mass transfer modeling for Cu/water and CuO/water nanofluid. *Adv Mech Engng*. 2013; p. 1–7.
  19. Bachok N, Ishak A, Pop I. Stagnation-point flow over a stretching/shrinking sheet in a nanofluid. *Nanoscale Res Lett*. 2011; 6:1–10.
  20. Oztop HF, Abu-Nada E. Numerical study of natural convection in partially heated rectangular enclosures filled with nanofluids. *Int J Heat Fluid Flow* 2008; 29:1326–36.
  21. Bachok N, Ishak A, Pop I. Stagnation point flow towards a stretching/shrinking sheet with a convective surface boundary condition. *J Franklin Inst*. 2013; 350:2736–44.
  22. Zaimi K, Ishak A. Stagnation-point flow and heat transfer over a non-linear stretching/shrinking sheet in a micropolar fluid. *Abs. Appl. Analysis*. 2014; p. 1–6.